Journal of
Chemical Engineering & Process Technology

Pirbazari, J Chem Eng Process Technol 2017, 8:2
DOI: 10.4172/2157-7048.1000333

Research Article Open Access

Photocatalytical Treatment of Synthetic Wastewater Containing Chlorophenols by TiO_2 Nanoparticles Sensitized with Cobalt Phthalocyanine Under Visible Light

Azadeh Ebrahimain Pirbazari*

Fouman Faculty of Engineering, College of Engineering, University of Tehran, Iran

Abstract

In this paper, sensitization TiO_2 nanoparticles with sulphonated cobalt phthalocyanine(CoPcS-TNP) has been reported. The prepared samples characterized by different analysis such as: XRD, FT-IR, EDX, nitrogen physisorption, TG and TEM techniques. The XRD, TEM and nitrogen physisorption results showed the prepared samples containing only the pure anatase phase with crystal sizes in the range of 7-10 nm and high surface areas of 133-280 m^2/g. The presence of CoPcS in photocatalysts confirmed by FT-IR and EDX analysis. The CoPcS-TNP samples showed efficient activity for photocatalytic degradation of 4-chlorophenol (4-CP) and 2,4-dichlorophenol (2,4-DCP) under visible light. The sample CoPcS-TNP (2.24) was the best photocatalyst for degradation of chlorophenols under visible light. The degradation reactions follow first-order kinetics. Reusing experiments of the photocatalyst showed a reduction activity from 95% to 60% for chlorophenols degradation after four cycles. The major intermediates of degradation were oxalic acid, pyruvic acid and malonic acid which identified by gas chromatography-mass spectrometry (GC/MS).

Keywords: TiO_2; Nanoparticles; Phthalocyanine, Degradation; Chlorophenols

Introduction

The production and usage of chemicals in industry has led to the entry of many xenobiotics into the environment. Chlorophenols (CPs) are used as flea repellents, fungicides, wood preservatives, fungus inhibitors, antiseptics, disinfectants and antigumming agents for gasoline during the industrial production of pesticides, herbicides, dyes, pigments, phenolic resins and paper. Also, some. Wastewater of paper and pesticides industries contains chlorophenols [1-3]. The widespread occurrence of phenols in wastewater and associated environmental hazards has heightened concern over public health [4].

Activated carbon adsorption, membrane filtration, chemical coagulation, ion exchange on synthetic adsorbent resins are the conventional wastewater purification systems that generate secondary wastes during the treatment of contaminated water, which requires additional steps and cost. Heterogeneous photocatalytic oxidation (HPO) process as a promising new route for the degradation of persistent organic pollutants, employing TiO_2 and UV light has emerged, and produced more biologically degradable and less toxic substances [5,6]. This process is largely dependent on the *in-situ* generation of hydroxyl radicals under ambient conditions which are capable of converting a wide spectrum of toxic organic compounds including the non-biodegradable ones into relatively innocuous end products such as CO_2 and H_2O. Destruction of recalcitrant organics in the HPO process, is governed by the combined actions of an energetic radiation source, an oxidizing agent and a semiconductor photocatalyst [7]. The sun produces 0.2-0.3 mol photons m^{-2} h^{-1} in the range of 300-400 nm with a typical UV flux of 20-30 Wm^2 near the earth's surface, this suggests using sunlight as an economically and ecologically sensible light source [8]. Many attempts have been made to develop of an efficient wastewater treatment process for large scale applications have received considerable attention. Recently photocatalytic degradation of phenol and substituted phenols in wastewater has been widely investigated. Several reviews [9,10] focusing briefly on the available technologies for the abatement of phenolic compounds in wastewater have recently been published. TiO_2-type semiconductor photocatalysts have attracted considerable attention because of their good physicochemical stability and their ability to catalyze the effective elimination of organic refractory contaminants from the aquatic environment [7,11-14]. The main focus of the recent TiO_2 photocatalysis research is How to improve the photocatalytic efficiency of TiO_2 in the visible region? [15,16]. Researches have been made to achieve the utilization of visible light for TiO_2 material, such as transitional metal ion doping [17-19], nonmetal element doping [20,21] and dye sensitization [22,23]. In the dye-sensitized photocatalysis process, the dye absorbs the light and a subsequent electron transfer from the excited state of the dye to the conduction band of TiO_2 semiconductor. The electron transferring from excited state of the dye to the conduction band of TiO_2 depends strongly on the adsorption property of dye molecules [24]; and by the competitive adsorption of other coexisting species in the solution.. Because of low cost and efficiency relative to the conventional solid-state conversion of visible light into chemical energy, the use of phthalocyanines and porphyrins has attracted significant attention. The main steps in a photocatalytic process based on TiO_2-phthalocyanine nanoparticles can be described as below [25]:

(1) A macrocycle compound attached to the TiO_2 surface absorbs visible light, thereby

(2) Promoting electron injection into the TiO_2 conduction band.

(3) direct oxidation of the organic compound

(4) Internal cross systems processes at the excited dye

***Corresponding author:** Azadeh Ebrahimain Pirbazari, Fouman Faculty of Engineering, College of Engineering, University of Tehran, Iran, Tel: 981334734927; E-mail: aebrahimian@ut.ac.ir

Received April 11, 2017; **Accepted** April 18, 2017; **Published** April 29, 2017

Citation: Pirbazari AE (2017) Photocatalytical Treatment of Synthetic Wastewater Containing Chlorophenols by TiO_2 Nanoparticles Sensitized with Cobalt Phthalocyanine Under Visible Light. J Chem Eng Process Technol 8: 333. doi: 10.4172/2157-7048.1000333

(5) Singlet oxygen produced by the interaction of dye in an excited triplet state with molecular oxygen

(6) Reduction of dissolved oxygen produced hydroxyl radical, hydroxyl anion and singlet oxygen

(7) Superoxide radical reacts with the sensitizer cation and produced hydroxyl radical

(8) Singlet oxygen reduced at the sensitizer and produced hydroxyl radical

(9) Environmental global reaction: organic compound oxidation by the two main oxidants: hydroxyl radicals and singlet oxygen.

To the best of knowledge, there is some works have been devoted to the characteristics and application of TiO_2 nanoparticles containing phthalocyanines and in these reports the photocatalysts prepared by the impregnation method [26-30]. A common disadvantage of this method is a low degree of molecular distribution of the dye molecules in the TiO_2 structure. Incorporation of phthalocyanines into TiO_2 gel has also been reported [31-33]. Due to the incomplete characterization and uncertain validation of the photocatalytic activity mechanism, complementary study is still needed. The enhanced photocatalytic activity of TiO_2 sentisized by iron (III) phthalocyanine has been ascribed to the effective formation of hydroxyl radicals generated from both components [31]. The photocatalytic activity of TiO_2 containing copper phthalocyanine has been assigned to a dye-sensitized TiO_2 photocatalytic mechanism [33]. Although this photocatalyst functions under visible light but it cannot achieve complete degradation of methyl orange as a model pollutant. The aim of this work is, preparation of TiO_2 nanoparticles containing different amounts of sulphonated cobalt phthalocyanine (CoPcS) by the hydrothermal method. The prepared samples were characterized by different analysis and used for the heterogeneous photocatalytic degradation of 4-chlorophenol (4-CP) and 2,4-dichlorophenol (2,4-DCP) under visible light, which revealed enhanced photocatalytic activity as compared to the pure TiO_2. The kinetic of chlorophenols degradation were investigated and the reaction intermediates during degradation were identified by GC-MS analysis.

Experimental

Materials and reagents

Cobalt phthalocyanine complex (CoPc) was purchased from (Alfa Aesar No. A16658). The sulphonated form of complex was obtained by a conventional procedure [34]. Sulphonation of CoPc carried out by chlorosulfuric acid, $HClSO_4$ (Fluka No. 26388). Tetraisopropylorthotitanat (Merck No. 8.21895), ethanol, acetylacetone and deionized water were used for photocatalyst synthesis. High-purity 4- chlorophenol(4-CP) (Merck No. 802254) and 2,4-dichlorophenol (2,4-DCP) (Merck No. 803774) were used as a model of organic pollutant for photocatalytic tests. H_2O_2 (Merck No. 1.08597) was used as accelerating oxidant in the photocatalytic tests.

Cobalt phthalocyanine sulphonation

According to reported procedure in Ref. [34], 0.5 g of CoPc and 25 mL $HClSO_4$ were treated and the mixture was heated to 150°C for 2 h. The resultant slurry was quenched over crushed ice. A deep blue solid was isolated by suction filtration and hydrolyzed to yield CoPcS. This compound was characterized by UV-Vis spectroscopy.

Photocatalyst synthesis

TiO_2 nanoparticles containing different amounts of CoPcS and pure TiO_2 were synthesized by the described procedure in Ref. [33]. 20 mL $Ti(OC_3H_7)_4$, 20 mL ethanol and 1.62 mL acetylacetone was prepared and stirred for 30 min at room temperature (solution A). Then, a new mixture (solution B), containing X mg CoPcS (X: 30, 60, 120 and 180 mg), 80 mL ethanol and 2 mL H_2O was added into the solution A, which led to a coloured solution. This solution was transferred into an autoclave, and then heated to 240°C at a heating rate of about 2°C min^{-1}. Finally, the temperature was kept at 240°C for 6 h. After cooling, the obtained solid washed with ethanol and water and dried at 150°C for 2 h in air. From now on, these photocatalysts are labelled as CoPcS-TNP(x), where (x) is the nominal weight percentage of CoPcS in the final solid. A solution without CoPcS was also preparedto obtain a control sample. This photocatalyst contains only TiO_2 prepared by an identical procedure.

Characterization

A Siemens D500 automatic diffractometer with a Cu K_α monochromatized radiation source was used for recording of the X-ray diffraction (XRD) patterns of various solid phases. The peak intensities were fitted by a pseudo-Voigt function assuming a linear background. The standard error was ~ ± 5%. Transmission electron microscopy (TEM) studies were carried out with a Hitachi-H- 8100 instrument (accelerating voltage up to 200 kV, LaB6 filament). The samples were prepared by dispersing in an ultrasonic bath for 20 min in ethanol. The nitrogen physisorption measurements were carried out with a Quantachrome Autosorb-1-MP. The BET areas were determined by static nitrogen physisorption at ~196°C subsequent to out-gassing at 180°C, until the pressure was lower than 5 mbar. Diffuse reflectance spectra were recorded with a Perkin Elmer Spectrophotometer equipped with an integrating sphere assembly. The spectra were recorded at room temperature against barium sulphate. Fourier-transform infrared (FT-IR) spectra were recorded with a Shimadzu FT-IR spectrometer (Model 8400). Elemental chemical analysis (Vario EL, Elementar) was performed to determine the carbon and sulphur contents of the samples. The thermogravimetric analyses of the samples were carried out with a Cahn TG 2131 thermobalance in the temperature range of 25-900°C at a heating rate of 5°C/min in 100% pure helium. The reaction intermediates were identified by GC-MS in an Agilent 190915-433 instrument equipped with a HP-5MS capillary column (30 m × 0.25 mm). The column temperature was programmed at 50°C for 2 min, and from 50 to 250°C at a rate of 10°C min^{-1}. The samples used for GC-MS analysis were prepared according to the following procedure: The obtained degradation product was acidified to pH 1 and subsequently extracted with dichloro-methane. After dichloromethane was evaporated to dryness under vacuum, 10 mL methanol was added to dissolve the residue. Then, 1 mL concentrated sulfuric acid was added and the combined solution was refluxed for about 3 h. The solution was further extracted with dichloromethane followed by concentrating to about 1 mL under reduced pressure. The released chloride ions originating from the degradation of chlorophenols were identified and determined by the $AgNO_3$ method.

Photocatalytic degradation of chlorophenols

The photcatalytic activity of prepared photocatalysts was investigated for degradation of chlorophenols. The suspension containing optimum dose of photocatalyst and 50 mL aqueous solution of each chlorophenols (Conc: 40 mg/L) was stirred first in the dark for 10 min to establish adsorption/desorption equilibrium. Irradiation experiments were carried out in a self-built reactor. In some experiments, H_2O_2 (as an oxidant) was also added to the solution before

light irradiation. A visible (Halogen, ECO OSRAM, 500W) lamp was used as irradiation source. At certain intervals, small aliquots (2 mL) were withdrawn and filtered to remove the photocatalyst particles. These aliquots were used for monitoring the degradation progress, with Biochrom WPA, Biowave II spectrophotometerat λ_{max}=224 nm.

Results and Discussion

Characterization of synthesized photocatalysts

X-ray diffraction analysis: The XRD patterns of synthesized samples were shown in Figure 1. The patterns indicated that TiO_2 nanoparticles and the CoPcS-TNP samples consist of the pure anatase phase (PDF 24-1272). The XRD patterns showed that presence of CoPcS complex into TiO_2 structure didn't change the diffraction positions and lattice parameters of TiO_2 (Figure 1). The diffraction patterns of pure TiO_2 and CoPcS-TNP samples shown considerable line width, indicating small crystal. Based on the Scherrer equation, the crystal size of the prepared photocatalysts can be calculated from the width of the anatase (101) diffraction width. The crystallite dimensions were determined using the equation:

$$D_{(hkl)}=0.9\,\lambda/\,\beta\,\mathrm{Cos}\,\theta \quad (1)$$

Where $D_{(hkl)}$ is the crystal thickness in the h k l direction, λ is the wavelength of the X-ray radiation, β is the peak width at half-maximum corrected for instrumental broadening, and θ is the Bragg angle of the diffraction peak. The crystal size of the pure TiO_2 and CoPcS-TNP photocatalysts are in the range from 7.5 to 9.5 nm (Table 1).

Diffuse reflectance spectroscopy: The diffuse reflectance spectra of the synthesized samples are shown in Figure 2. Pure TiO_2 has no significant absorbance in the visible region because of the large band gap energy (3.1 eV), and exhibits only a fundamental absorption band in the UV region (Figure 2a). The diffuse reflectance spectra of CoPcS-TNP samples exhibit absorption bands in the 600-700 nm regions (Figure 2b-2e). The two maxima in the visible region correspond to the Q absorption bands originating from $\pi\rightarrow\pi^*$ transitions of CoPcS, which demonstrate that the absorption spectra of CoPcS-TNP samples extend to the visible region. The monomeric and aggregated form of CoPcS complex exhibited the absorption bands at about 680 and 620 nm, respectively [35]. The band gap energy was calculated from the DR spectra according to below equation [36] for the pure TiO_2 and CoPcS-TNP samples.

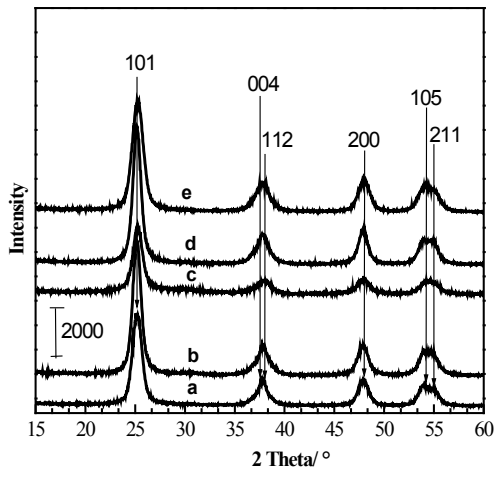

Figure 1: Powder XRD patterns of (a) TiO_2, (b) CoPcS-TNP (0.56), (c) CoPcS-TNP (1.12), (d) CoPcS-TNP (2.24) and (e) CoPcS-TNP (3.36).

Sample	Phase	Crystal Size (nm)
TiO_2	Anatase	9.0
CoPcS-TNP (0.56)	Anatase	9.0
CoPcS-TNP (1.12)	Anatase	8.0
CoPcS-TNP (2.24)	Anatase	9.5
CoPcS-TNP (3.36)	Anatase	7.5

Table 1: Crystalline phase and crystal size identified by XRD.

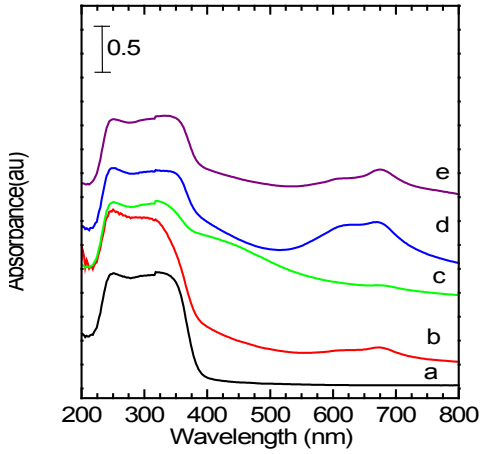

Figure 2: Diffuse reflectance spectra of (a) TiO_2, (b) CoPcS-TNP (0.56), (c) CoPcS-TNP (1.12), (d) CoPcS-TNP (2.24) and (e) CoPcS-TNP (3.36).

$$E_{bg}=1240/\lambda \quad (2)$$

Where E_{bg} is the band gap energy (eV) and λ is wavelength (nm) obtained from the DR spectra. The E_{bg} data and the colour of samplesare summarized in Table 2. The band gap energy for all the samples except CoPcS-TNP (1.12) are within 3.10-3.11 eV. The lower band gap energy of 2.97 eV observed for CoPcS-TNP (1.12) may be due to the very low degree of incorporation of CoPcS into TiO_2. It may be concluded part of CoPcS molecules have been decomposed during the hydrothermal synthesis, and some of the cobalt species were inserted into the TiO_2 bulk decreasing the band gap energy.

FT-IR spectroscopy: The FT-IR spectra of the CoPcS, pure TiO_2 and CoPcS-TNP (2.24) sample are shown in Figure 3a and Figure 3b Some of the characteristic bands of CoPcS (Figure 3c) appeared in the 1700-1000 cm^{-1} regions [37]. The spectrum b in Figure 3 originates from the CoPcS-TNP (2.24) sample. The vibration about 1400 cm^{-1} can be attributed to cobalt phthalocyanine species in the synthesized photocatalysts [38], which is labelled with an asterix in Figure 3. The intensity of the 1400 cm^{-1} vibration is weak, because the amount of CoPcS incorporated into TiO_2 is low. The vibrations at about 670 cm^{-1} (Figure 3c) due to the sulfonic groups of CoPcS [39] disappeared in the CoPcS-TNP (2.24) sample, which is most likely due to the formation of $TiO\text{-}SO_3^-$ bond (Figure 4). Covalent grafting of sulphonated iron (III) phthalocyanine onto TiO_2 nanoparticles was carried out by Sorokin et al. [40] through sol-gel procedure. Their obtained characterization results showed that sulfonic groups are chemisorbed onto the TiO_2 nanoparticles and sulphonated iron (III) phthalocyanine complex acts as a bridging ligand and controls the molecular self-assembly hydrolytic process. Recently Núñez and etal reported modification of TiO_2 surface with copper(II) phthalocyanine-tetrasulfonic acid tetrasodium (CuPc-ulfunic acid) and their FT-IR data showed, the S-O-Ti characteristic stretching signals at 1150 and 1210 cm^{-1} suggest chemisorptions of CuPc complex through acid bond formation ($TiO\text{-}SO_3^{-}$) between Ti-OH and

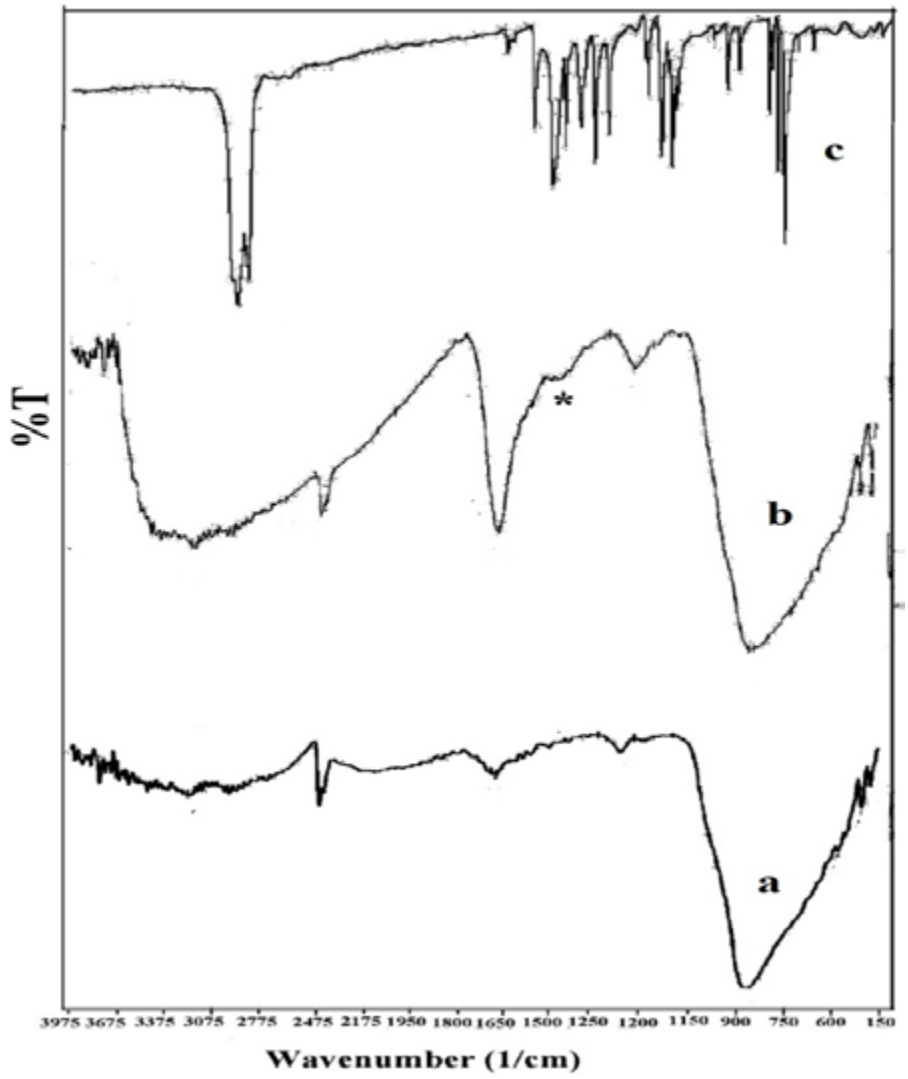

Figure 3: FT-IR pactra of a) TiO_2, b) CoPcS-TNP (2.24) and c) CoPcS.

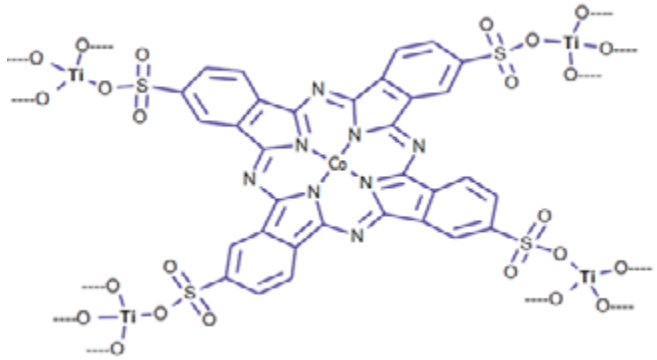

Figure 4: Chemical CoPcS adsorption on the TNP surface.

CuPc-sulfonic [25]. Their adsorption isotherm investigation showed that each CuPc molecules adsorbed onto TiO_2 surface nanoparticles using two or more sulfonic acid moieties. Therefore, the CuPc molecules may have more planar distribution on the TiO_2 surface and prevents CuPc molecule multi anchoring at the TiO_2 surface [25].

Sample	Colour	λ (nm)	Band gap energy (eV)
TiO_2	White	399	3.11
CoPcS-TNP (0.56)	Green	399	3.11
CoPcS-TNP(1.12)	Yellow	418	2.97
CoPcS-TNP(2.24)	Dark Green	400	3.10
CoPcS-TNP (3.36)	Pale blue	400	3.10

Table 2: Colour, wavelength and band gap energy of the prepared samples.

Transmission electron microscopy (TEM): The particle size and morphology of the prepared samples were analyzed by TEM. The TEM micrographs (Figure 5) revealed that the samples consist of nanoparticles with diameters in the range from 7 to 10 nm. The samples are not agglomerated, which is useful to increase the photocatalytic activity of the prepared samples. The chemical analysis results are summarized in Table 3. The obtained data from sulfur content suggest an average of two sulphonate groups per CoPc complex. Also the carbon amount is relatively high for CoPcS-TNP (1.12) that may be indicated

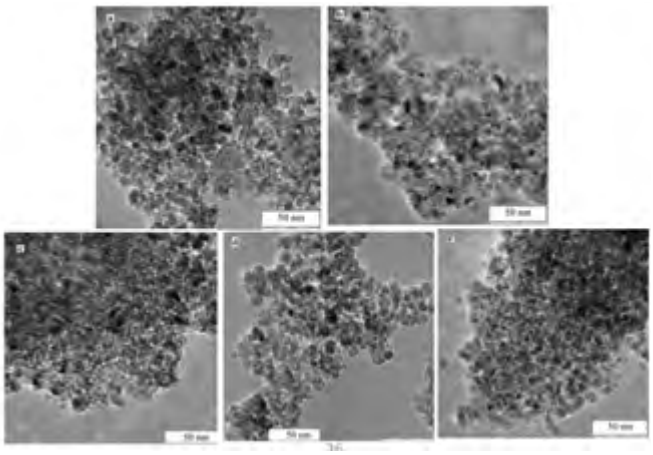

Figure 5: TEM micrograph of (a) TiO_2, (b) CoPcS-TNP (0.56), (c) CoPcS-TNP (1.12), (d) CoPcS-TNP (2.24) and (e) CoPcS-TNP (3.36).

Sample	%S	%C
TiO_2	0.00	1.14
CoPcS-TNP (0.56)	<0.10	1.87
CoPcS-TNP (1.12)	0.10	6.45
CoPcS-TNP (2.24)	0.20	2.04

Table 3: Elemental chemical analysis of the prepared samples.

decomposition of CoPcS complex during the hydrothermal synthesis and fractions of other organic compounds (such as acetylacetone or ethanol) remained as separated phase.

N_2 adsorption-desorption: Figure 6 shows N_2 adsorption-desorption isotherms of the pure and CoPcS-TNP samples. The sorption isotherms for all of the samples except CoPcS-TNP (1.12) correspond to the type IV isotherm according to the IUPAC classification [41]. Textural and structural parameters of the CoPcS-TNP samples are summarized in Table 4. Specific surface areas were calculated according to the BET method, pore volumes, and radii were derived from the desorption branch according to the BJH model. The specific surface areas of the CoPcS-TNP samples are lower than that of pure TiO_2 suggesting that incorporation of the CoPcS complex reduces the surface area of TiO_2 nanoparticles. Reduction of the surface area for CoPcS-TNP samples does not involve distortion of the TiO_2 crystal structure as shown by XRD analysis.

Thermogravimetric analysis: Thermogravimetric analysis curves of the prepared samples in helium atmosphere are shown in Figure 7. In the thermogram for pure TiO_2, three weight loss stages can be observed. The first weight loss is at about 90°C, which corresponds to desorption of physically adsorbed species such as H_2O and CO_2. The second weight loss at about 250°C is ascribed to the removal of hydroxyl groups from the surface of TiO_2 [42]. The third weight loss at about 370°C is for organic species decomposition, which used for preparation of TiO_2. We also observed three weight loss stages in the thermograms of the CoPcS-TNP samples (Figure 7). The first and the second weight loss at about at 90 and 370°C can again be attributed to desorption of water and decomposition of organic species, respectively. However, a new weight loss starting at about 500°C for CoPcS-TNP (2.24) and CoPcS-TNP (3.36) can be attributed to the decomposition of CoPcS complex. The phthalocyanines and their metallo derivatives are stable up to 400°C [43]. These results may indicate that CoPcS molecules immobilized onto TiO_2 nanoparticles through covalent bonding are more stable and decomposed at higher temperature (Figure 4). We did not observe dehydroxylation weight loss for CoPcS-containing TiO_2 samples at 250°C. This also is an indication of the strong interaction between TiO_2 and CoPcS through hydroxyl groups.

Photocatalytic degradation of chlorophenols

The photocatalytic efficiency of the CoPcS-TNP samples was investigated for degradation of chlorophenols. Elimination time of chlorophenols in the presence of the prepared photocatalysts is shown in Table 5. All of the CoPcS-TNP samples are more efficient in the degradation of chlorophenols compared to pure TiO_2, and the degradation rate of chlorophenols is the highest in presence of CoPcS-TNP (2.24). Obtained results can be confirmed the role of CoPcS complex as sensitizer on the surface of TNP: By the photon absorption, the electrons in the ground state of CoPcS complex are excited and then injected into the conduction band of TiO_2. Highly active species such as $OH^{\bullet}$ and $O_2^{\bullet-}$ are generated at the TiO_2 surface, where the photoelectrons and holes become effectively separated. The aggregated form of the CoPcS complex shortens the excited triplet state lifetimes by enhancement of internal conversion and therefore reducing their photosensitizing efficiency [44]. Consequently, a monomolecular distribution of the dye on the TiO_2 surfaces favors improved photocatalytic activity.

Figure 8 show the photocatalytic degradation of 4-CP (Figure 8a) and 2,4-DCP (Figure 8b) under various conditions and in the presence of the best photocatalyst (CoPcS-TNP (2.24)) respectively. Control experiments showed that the optimal dosage of photocatalyst is 0.3 g L^{-1}, and t a H_2O_2 concentration of 0.01 mol L^{-1} is adequate for photocatalytic degradation of chlorophenols. Complete elimination of 4-CP and 2,4-DCP are possible within 90 and 180 min in the presence of the CoPcS-TNP (2.24), H_2O_2, and visible light. Thus, the enhancement of the catalytic activity observed for the CoPcS-TNP samples compared to pure TiO_2 can be demonstrated synergetic effect of the sensitizer (CoPcS complex). CoPcS complex has a strong absorption around 600-650 nm (Figure 2), it has strong Q-band absorption and it can be excited under visible light. The excited CoPcS molecules inject electrons to the conduction band (CB) of TiO_2, the CB acts as a mediator and transfer electron acceptors on the TiO_2 surface, the valence band (VB) remains unaffected.

In the presence of hydrogen peroxide the activity of the photocatalyst may even be better (Figure 8). Almost 50% of 4-CP and 2,4-DCP are

Sample	SBET (m^2/g)	Pore radius (A˚)	Pore volume (cm^3/g)
TiO_2	280	19	0.24
CoPcS-TNP (0.56)	133	35	0.26
CoPcS-TNP (1.12)	208	9	0.14
CoPcS-TNP (2.24)	141	38	0.29
CoPcS-TNP (3.36)	197	18	0.17

Table 4: Textural and structural parameters of the prepared samples.

Sample	4-CP elimination time (min)	2,4-DCP elimination time (min)
TiO_2	180	360
CoPcS-TNP (0.56)	150	330
CoPcS-TNP (1.12)	130	300
CoPcS-TNP (2.24)	90	180
CoPcS-TNP (3.36)	110	240

Table 5: Elimination time of chlorophenols in presence of the prepared samples.

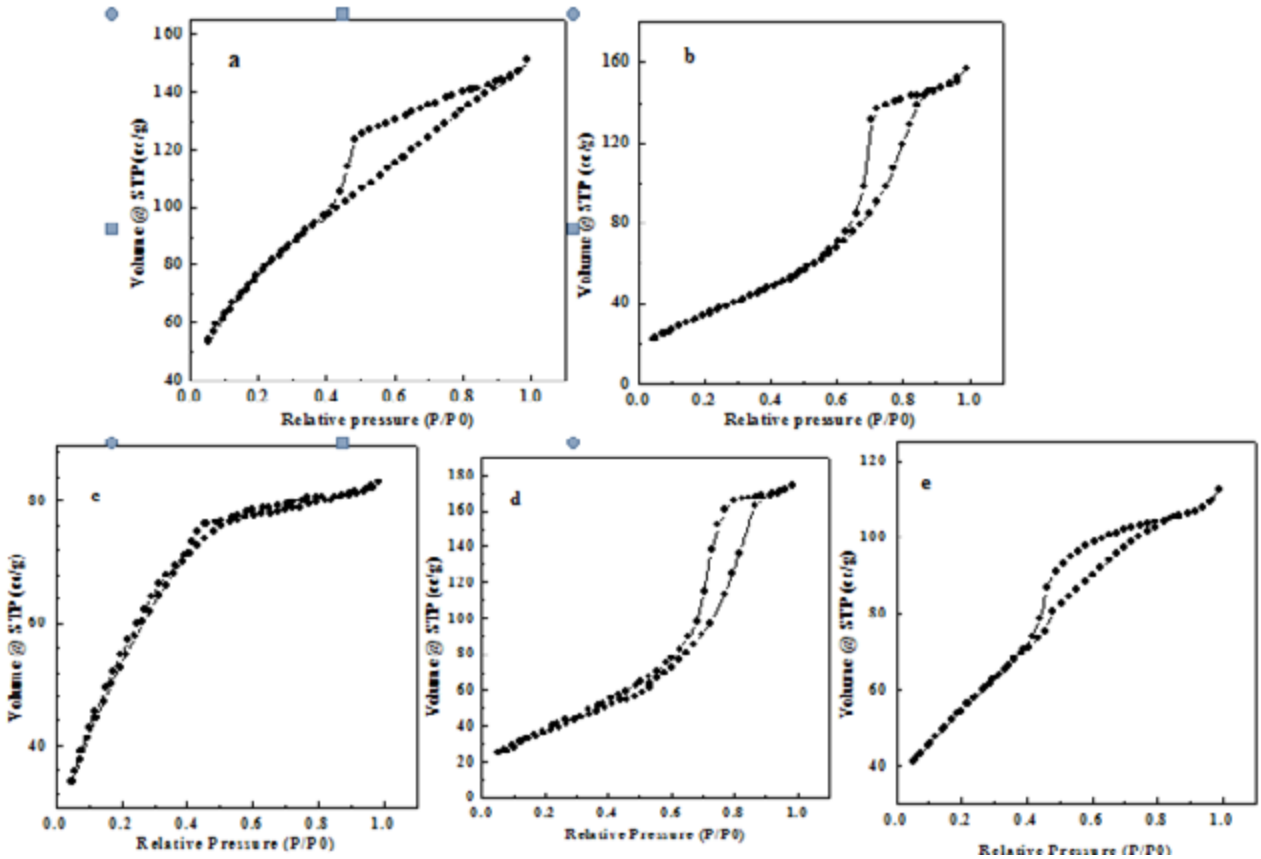

Figure 6: N_2 adsorption–desorption isotherms for (a) TiO_2, (b) CoPcS-TNP (0.56), (c) CoPcS-TNP (1.12), (d) CoPcS-TNP (2.24) and (e) CoPcS-TNP (3.36).

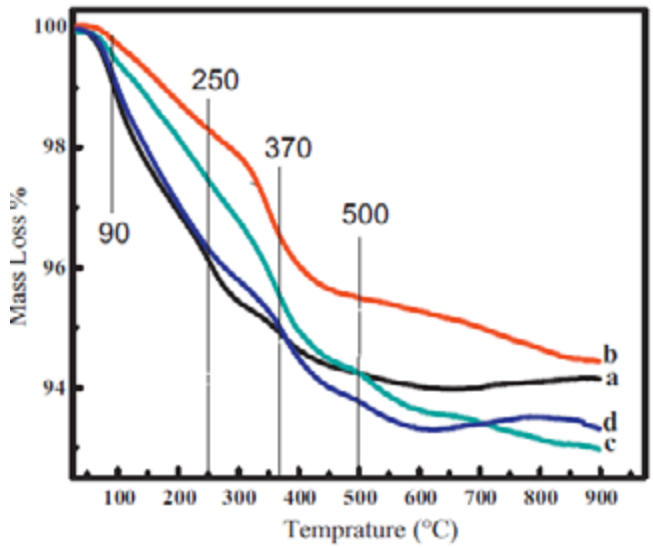

Figure 7: TG curves of (a) TiO_2, (b) CoPcS-TNP (0.56), (c) CoPcS-TNP (2.24) and (d) CoPcS-TNP (3.36).

degraded within 90 and 180 min, when there is no H_2O_2 added. More hydroxyl radicals are produced in the presence of H_2O_2 according to the below reaction:

$$H_2O_2+O_2^{\cdot-}\rightarrow OH^{\bullet}+OH^{-}+O_2 \quad (3)$$

This photocatalyst did not exhibit any photoactivity in the dark, neither in the absence nor in the presence of H_2O_2 (Figure 8), suggesting that it is necessary to photoexcite the sensitizer (CoPcS). The hydroxyl radicals are responsible for the degradation of the chlorophenols, yielding some intermediate compounds and mineralization products. The hydroxyl radical production was checked by Gao et al. proposed method [45,46], based on Nash's method [47]. It noticed that the production of hydroxyl radicals would produce a yellow color owing to the synthesis of diacetyldihydrolutidin [47]. The yellow color was observed when photocatalyst, H_2O_2 and the radiation were employed and the intensity of the color increased with increasing the time of irradiation. According to equation 3, the production of the hydroxyl radicals depends on the presence of superoxide radicals [46], therefore, the observation may suggest that the superoxide radicals are involved. During the photocatalytic degradation of chlorophenols, hydrogen peroxide could react with superoxide radicals to generate hydroxyl radicals.

GC/MS analysis: To obtain information about intermediates species formed during chlorophenols degradation process, GC/MS technique was employed. Figure 9 and Table 6 give major reaction intermediates containing carboxylic acid functional species. Formation of these intermediates can be explained as: After hydroxyl radiacals formation, the hydroxyl radicals attack to chlorophenols, converting them to chlorocatechol and then to chlorobenzoquinone, then hydroxyl radicals break the aromatic ring of chlorobenzoquinone, transferring them into simple acids like oxalic acid and acetic acid as the final products [48-50]. Chaliha and et al. [49] and Bian et al. [50] identified

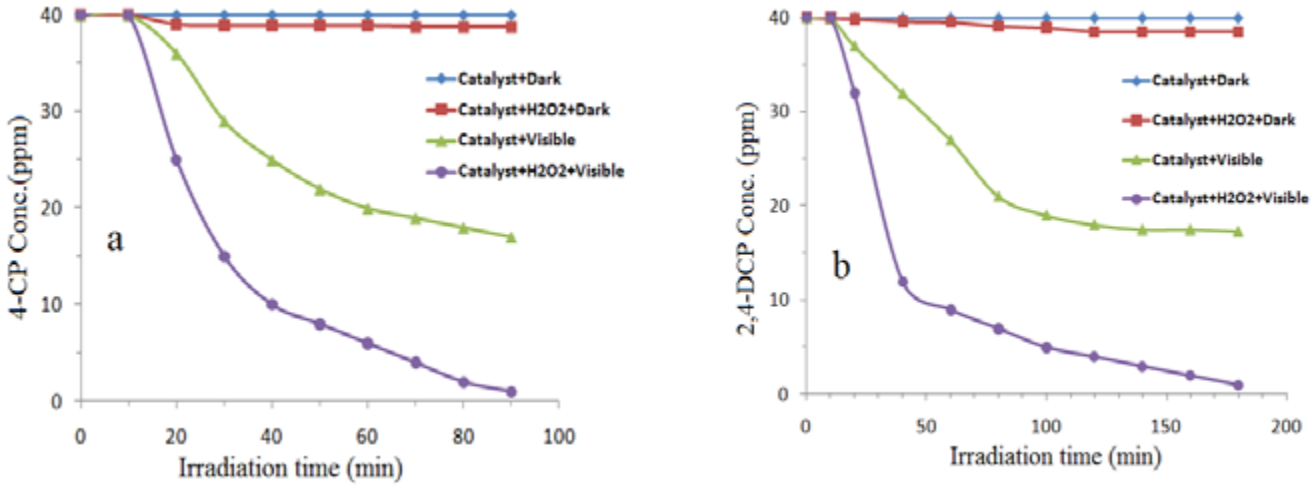

Figure 8: Concentration changes of a) 4-CP and b) 2, 4-DCP at various conditions.

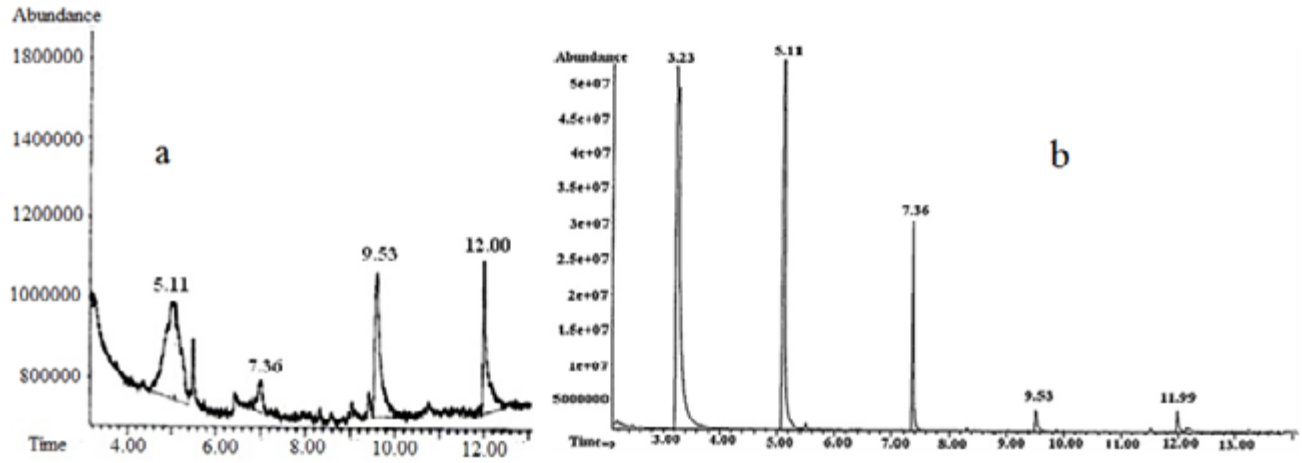

Figure 9: Chromatogram of the final products of the photocatalytic degradation of a) 4-CP and b) 2, 4-DCP by CoPcS-TNP (2.24).

Retention time (min)	Identified intermediate	Molecular formula
3.23	Methyl pyruvate	$H_3CCOCOOCH_3$
5.11	Methyl oxalate	$H_3COOCCOOCH_3$
7.36	Dimethyl malonate	$H_3COOCCH_2COOCH_3$

Table 6: The main intermediates of chlorophenols degradation determined by GC/MS.

the main ring-opened products resulting from 4-CP degradation by GC/MS and discussed the formation mechanism of them. In the proposed mechanism by Chaliha et al. [49], an electrophilic OH radical adds onto the 4-CP ring at an ortho- or para-position, leading to the formation of chlorocatechol and hydroquinone. On further oxidation, chlorocatechol is likely to be converted to aliphatic acids and hydroquinone to p-benzoquinone, which is easily oxidized to the corresponding dicarboxylic acid, 2,5-dioxo-3-hexenedioic acid. This acid produces maleic acid, which decomposes to oxalic acid, formic acid, acrylic acid, malonic acid and acetic acid. If there are no additional radical competitors in the solution, these low molecular weight organic acids can gradually be mineralized to carbon dioxide, the ultimate oxidation product. Also, a number of the intermediates identified in this work (Table 6) are in agreement with those reported in ref [51]. Benzoic acid formation with higher carbon compare chlorophenols can be illustrated according to the Rao et al. report (Figure 10) [52]. They proposed that radical I and a chloride radical ($Cl^{\bullet}$) formed by homolytic cleavage of aryl-Cl bond or by interaction of 2-CP with electrons on the surface of TiO_2 [53]. In a second step, radical I may dimerize to yield [1,1'-biphenyl]-2,2'-diol or combine with formyl radical produced *in-situ* to give 4-hydroxybenzaldehyde and benzoic acid formed by oxidation of hydroxybenzaldehyde. Hydroxyl radicals can attack the aromatic moiety due to their electrophilic nature [54]. Progress of the photocatalytic degradation was detected by chloride ion measurement through $AgNO_3$ test method. The presence of Cl^- in the reaction media accounts up almost 100% for chlorophenols degradation if compared to the maximum achievable concentration.

Photocatalyst reuse: The stability of the anchored photocatalysts is very important for its application in environmental technology. Therefore, the effectiveness of photocatalyst reuse was examined for degradation of each chlorophenols during a four cycle experiment.

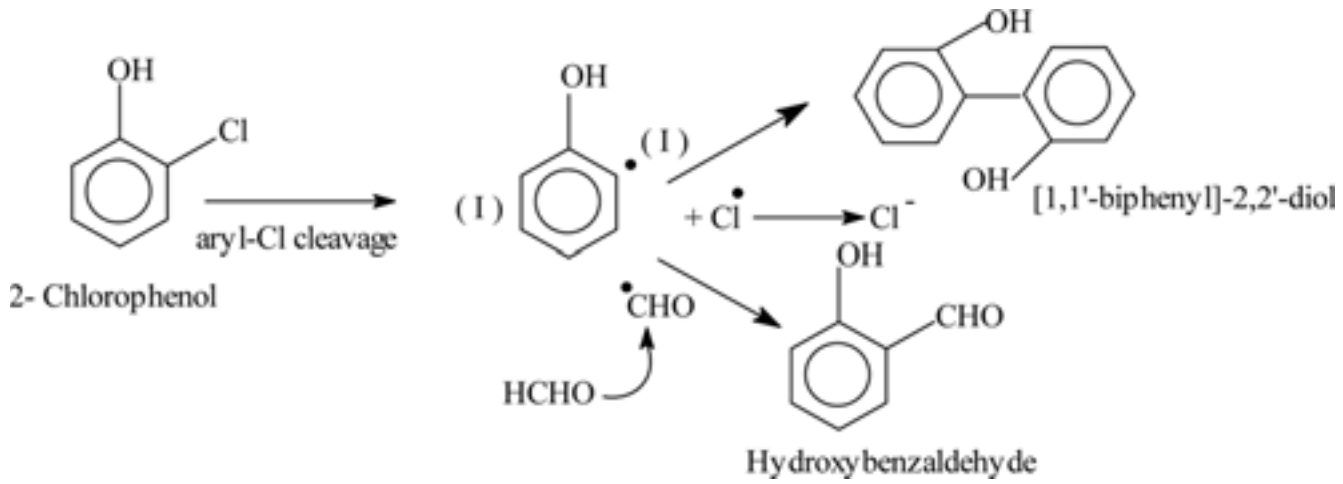

Figure 10: Rao proposed mechanism of formation of higher carbon intermediates [52].

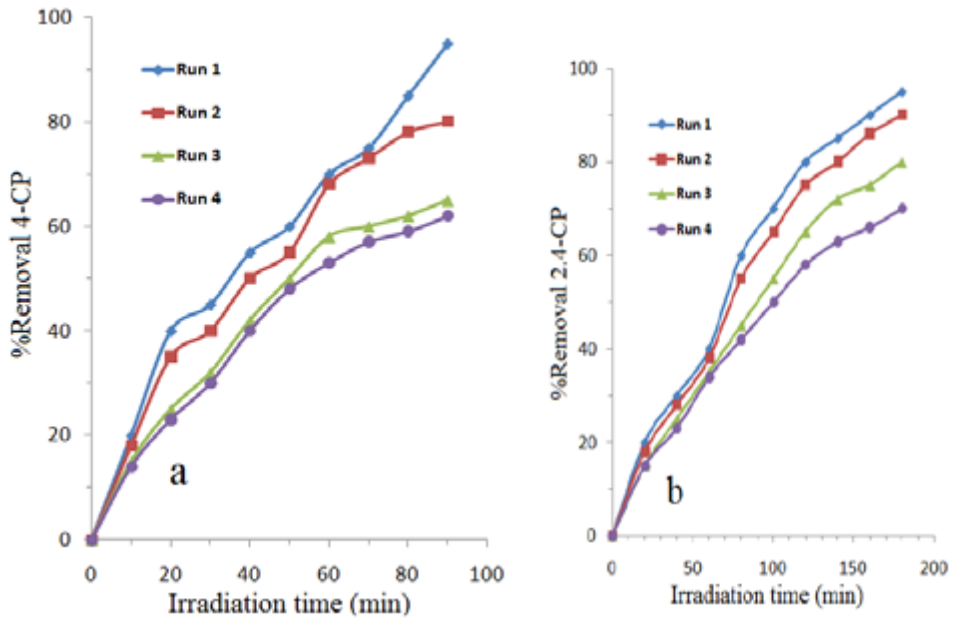

Figure 11: The recyclability of CoPcS-TNP (2.24) for a) 4-CP and b)2,4-DCP photocatalytic degradation for four successive cycles.

Each experiment was carried out under identical conditions (Figure 11). 50 mL of each chlorophenols with an initial concentration of 40 mg/L, 15 mg photocatalyst and 0.03 mol/L H_2O_2 and 90 and 180 min irradiation time under visible light were used. Recycling experiments showed a photocatalytic activity reduction from 95% to 60% after four catalytic cycles. The main reasons for reduction of photocatalytic activity are permanent adsorption of intermediate species or probable attack of OH radicals to the anchored phthalocyanine complex.

The effect of the initial concentration: The photocatalytic degradation of chlorophenols is a first-order reaction and and its kinetics may be expressed as $\ln(C_0/C)=k_{obs}t$. In this equation k_{obs} (min^{-1}) is the apparent rate constant, C_0 and C are the initial concentration and concentration at reaction time t of each chlorophenols, respectively. The k_{obs} are found from the slopes of the straight lines obtained by plotting $\ln(C_0/C)$ versus irradiation time. The reaction rates, rate constants and half-lifes ($t_{1/2}$) at various initial concentrations of each chlorophenols are given in Table 7. The results summarized in Table 7 show that the reaction rate of photocatalytic degradation of chlorophenols is faster at higher initial concentration. However, the rate constants decrease to some extent when the initial concentrations increase. The initial degradation rate of chlorophenols increased by increasing of chlorophenols concentration because the oxygen active species formed on the CoPcS surface have a limited lifetime and react with the chlorophenoles near the photocatalyst surface.

Conclusion

In this work, TiO_2 nanoparticles containing different amounts of CoPcS (CoPcS-TNP) were synthesized and characterized by different analysis such as: XRD, FTIR, TEM, TG, nitrogen physisorption and DRS. The nitrogen physisorption and FTIR analysis results indicate

4-CP				
Initial Conc. (µg/mL)	**kobs (min^{-1})**	**Reaction rate (µg/mL. min)**	**t1/2 (min)**	**R^2**
20	0.0539	1.1078	12.86	0.9985
30	0.0384	1.154	18.04	0.9992
40	0.0294	1.176	23.57	0.9995
60	0.0199	1.195	34.82	0.9989
80	0.0149	1.199	46.51	0.9991
2,4-DCP				
Initial Conc. (µg/mL)	**kobs (min^{-1})**	**Reaction rate (µg/mL. min)**	**t1/2 (min)**	**R^2**
20	0.0221	0.442	31.36	0.9986
30	0.0158	0.474	43.86	0.9975
40	0.0129	0.516	53.72	0.9965
60	0.0088	0.528	78.75	0.9991
80	0.0079	0.632	87.72	0.9978

Table 7: First-order reaction rate constants and correlation coefficients for different concentrations of chlorophenols.

that CoPcS molecules act as bridge ligand and attached on the surface of TiO_2 nanoparticles through SO_2-O-TiO_2 bonds. The CoPcS-TNP samples should contain an optimum amount of CoPcs anchored to the TiO_2 surfaces for better photocatalytic activity. The obtained results for degradation of chlorophenols showed that the incorporation of 2.24 wt% CoPcS provides the most photoactive sample. The kinetics of the reaction is first-order and the main intermediates of reaction identified by GC/MS.

Acknowledgements

The author wish to acknowledge the financial support of Iran National Science Foundation (Grant No: 92025598). Also, I am so thankful to University of Tehran for supporting of this research.

References

1. Peng JF, Liu JF, Hu XL, Jiang GB (2007) Direct determination of chlorophenols in environmental water samples by hollow fiber supported ionic liquid membrane extraction coupled with high performance liquid chromatography. J. Chromatogr. A 1139: 165-170.
2. Fukushima M, Tatsumi K (2001) Degradation pathways of pentachlorophenol byphoto-Fenton systems in the presence of iron (III), humic acid and hydrogenperoxide. Environ Sci Technol 35: 1771-1778.
3. Gonzalez LF, Sarria V, Sanchez OF (2010) Degradation of chlorophenols by sequential biological-advanced oxidative process using Trametes pubescens and TiO_2/UV. Bio Technol 101: 3493-3499.
4. Eriksson E, Baun A, Mikkelsen PS, Ledin A (2007) Risk assessment of xenobiotics in stormwater discharged to HarrestupAo, Denmark. Desalination 215: 187-197.
5. Oller I, Gernjak W, Maldonado MI, Perez ELA, Sanchez PJA, et al. (2006) Solar photocatalytic degradation of some hazardous water-soluble pesticides at pilot-plant scale. J. Hazard. Mater 138: 507-517.
6. Garcýa A, Amat AM, Arques A, Vicente R, Lopez MF, et al. (2007) Increased biodegradability of UltracidTMin aqueous solutions withsolar TiO_2 photocatalysis. Chemosphere 68: 293-300.
7. Ahmed S, Rasul MG, Martens WN, Brown R, Hashib MA (2010) Heterogeneous photocatalytic degradation of phenols in wastewater: A review oncurrent status and developments. Desalination 261: 3-18.
8. Goslich R, Dillert R, Bahnemann D (1997) Solar water treatment principles and reactors. Water Sci. Technol 35: 137-148.
9. Busca G, Berardinelli S, Resini C, Arrigi L (2008) Technologies for the removal ofphenol from fluid streams. A short review of recent developments J. Hazard. Mater 160: 265-288.
10. Liotta LF, Gruttadauria M, Di CG, Perrini G, Librando V (2009) Heterogeneous catalytic degradation of phenolic substrates: catalysts activity. J. Hazard. Mater 162: 588-606.
11. Augugliaroa V, Bellarditaa M, Loddoa V, Palmisanoa G, Palmisanoa L, et al. (2012) Overview on oxidation mechanisms of organic compounds by TiO_2 in heterogeneous photocatalysis. J. Photochem. Photobiol. C: Photochem. Rev 13: 224-245.
12. Gayaa UI, Abdullaha AH (2008) Heterogeneous photocatalytic degradation of organic contaminants overtitanium dioxide: A review of fundamentals, progress and problems. J. Photochem. Photobiol. C: Photochem. Rev 9: 1-12.
13. Agrios GA, Pichat P (2005) State of the art and perspectives on materials and applications of photocatalysis over TiO_2. J. Appl. Electrochem 35: 655-663.
14. Demeesterea K, Dewulf J, Van LH (2007) Heterogeneous photocatalysis as an advanced oxidation process for the abatement of chlorinated, monocyclicaromatic and sulfurous volatile organic compounds in air: State of the art. Crit. Rev. Environ. Sci. Technol 37: 489-538.
15. Pelaez M, Nolan NT, Pillai SC, Seery MK, Falaras P, et al. (2012) A review on the visible light active titanium dioxide photocatalysts for environmental applications. Appl. Catal. B: Environ. 125: 331-349.
16. Han F, Rao VS, Srinivasan M, Rajarathnam D, Naidu R (2009) Tailored titanium dioxide photocatalysts for the degradation of organic dyes in wastewater treatment: A review. Appl. Catal/ A: General 359: 25-40.
17. Choi W, Termin A, Hoffmann MR (1994) The role of metal ion dopants in quantumsizedTiO_2: correlation between photoreactivity and charge carrierrecombination dynamics. J. Phys. Chem 98: 13669.
18. Zhu J, Deng Z, Chen F, Zhang J, Chen H, et al. (2006) Hydrothermal doping method for preparation of Cr^{3+}-TiO_2 photocatalysts withconcentration gradient distribution of Cr^{3+}. Appl. Catal. B 62: 325-329.
19. Yuan S, Sheng Q, Zhang J, Chen F, Anpo M (2005) Synthesis of La^{3+} dopedmesoporoustitania with highly crystallized walls, Micropor. Mesopor. Mater 79: 93-99.
20. Asahi R, Morikawa T, Ohwaki T, Aoki K, Taga Y (2001) Visible-light photocatalysisin nitrogen-doped titanium oxides. Science 293: 269-271.
21. CongY, Zhang J, Chen F, Anpo M (2007) Synthesis and characterization of nitrogendopedTiO_2 nanophotocatalyst with high visible light activity. J. Phys. Chem. C 111: 6976-6982.
22. Bae E, Choi W, Park J, Shin HS, Kim SB et al. (2004) Effects of surface anchoringgroups (carboxylate vs. phosphonate) in ruthenium-complex-sensitized TiO_2on visible light reactivity in aqueous suspensions. J. Phys. Chem. B 108: 14093-14102.
23. Bae E, Choi W (2003) Highly enhanced photoreductive degradation of perchlorinatedcompounds on dye-sensitized metal/TiO_2 under visible light. Environ. Sci.Technol 37: 147-152.

24. Zhao J, Wu T, Wu K, Oikawa K, Hidaka H, et al. (1998) Photoassisteddegradation of dye pollutants. 3. Degradation of the cationic dye rhodamine Bin aqueous anionicsurfactant/TiO_2 dispersions under visible light irradiation: evidence for the need of substrate adsorption on TiO_2 particles. Environ. Sci.Technol. 32: 2394-2400.

25. Vargas E, Vargas R, Núñez O (2014) A TiO_2 surface modified with copper(II) phthalocyanine-tetrasulfonic acid tetrasodium salt as a catalyst during photoinduceddichlorvos mineralization by visible solar ligh. Appl. Catal. B: Environ. 156: 157 8-14.

26. Mele G, Del SR, Vasapollo G, Marci G, Garcia LE, et al. (2005) TRMC, XPS, and EPR characterizations of polycrystalline TiO_2 porphyrin impregnated powders and their catalytic activity for 4-nitrophenol photodegradation in aqueous suspension, J. Phys. Chem. B 109: 12347-12352.

27. Mele G, Del SR, Vasapollo G, Garcia LE, Palmisano L, et al. (2007) Photocatalytic degradation of 4-nitrophenol in aqueous suspension by using polycrystalline TiO_2impregnated with functionalized Cu(II)-porphyrin or Cu(II)-phthalocyanine Complexes. J. Catal. 117: 6581-6588.

28. Granados GO, Paez CAM, Martınez FO, Paez MEA (2005) Photocatalytic degradation of phenol on TiO_2 and TiO_2/Pt sensitized with metallophthalocyanines. Catal. Today 107: 589-594.

29. Li L, Xin B (2010) Photogenerated carrier transfer mechanism and photocatalysis properties of TiO2 sensitized by Zn(II) phthalocyanine. J. Central South University of Technol 17: 218-222.

30. Fa W, Zan L, Gong C, Zhong J, Deng K (2008) Solid-phase photocatalytic degradation of polystyrene with TiO_2 modified by iron (II) phthalocyanine. Appl. Catal. B: Environ 79: 216-223.

31. Ranjit KT, Willner I, Bossmann S, Braun A (1998) Iron(III) phthalocyanine-modified titanium dioxide: a novel photocatalyst for the enhanced photodegradation of organic pollutants. J. Phys. Chem. B 102: 9397-9403.

32. Wang Z, Mao W, Chen H, Zhang F, Fan X, et al. (2006) Copper(II) phthalocyaninetetrasulfonate sensitized nanocrystallinetitaniaphotocatalyst: synthesis in situ and photocatalysis under visible light. Catal. Commun. 7: 518-522.

33. Wang Z, Chen H, Tang P, Mao W, Zhang F, et al. (2006) Hydrothermal in situ preparation of the copper phthalocyaninetetrasulfonate modified titanium dioxide photocatalyst, Colloid. Surf. A: Physicochem. Eng. Aspects 289: 207-211.

34. Martin PC, Gouterman M, Pepich BV, Renzoni GE, Schindele DC (1991) Effects of ligands, solvent, and variable sulfonation on dimer formation of aluminum and zinc phthalocyaninesulfonates. Inorg. Chem. 30 3305-3309.

35. Iliev V, Alexiev V, Bilyarska L (1999) Effect of metal phthalocyanine complex aggregation on the catalytic and photocatalytic oxidation of sulfur containing compounds. J. Mol. Catal. A: Chem. 137: 15-22.

36. Kudo A, Miseki Y (2009) Heterogeneous photocatalyst materials for water splitting. Chem. Soc. Rev. 38: 253-278.

37. Seoudi R (2005) FTIR, TGA and DC electrical conductivity studies of phthalocyanine and its complexes. J. Mol. Struct 753: 119-126.

38. Karandikar P, Chandwadkar AJ, Agashe M, Ramgir NS, Sivasanker S (2006) Liquid phase oxidation of alkanes using Cu/Co-perchlorophthalocyanine immobilized MCM-41 under mild reaction conditions. Appl. Catal. A 297: 220-230.

39. Nabid MR, Asadi S, Shamsianpour M, Sedghi R, Osati S, et al. (2010) Oxidative polymerization of 3,4-ethylenedioxythiophene using transition-metal tetrasulfonatedphthalocyanine. React. Func. Polymers 70: 75-80.

40. Beyrhouty M, Sorokin AB, Daniele S, Hubert PLG (2005) Combination of two catalytic sites in a novel nanocrystalline TiO_2-iron tetrasulfophthalocyanine material provides better catalytic properties. NJ Chem 29: 1245-1248.

41. Sing KSW, Everett DH, Haul RAW, Moscou L, Pierotti RA (1985) Reporting physisorption data for gas/solid systems with special reference to the determination of surface area and porosity. Pure Appl. Chem. 57: 603-619.

42. Zhao Z, Fan J, Xie M, Wang Z (2009) Photo-catalytic reduction of carbon dioxide with in-situ synthesized CoPc/TiO_2 under visible light irradiation. J. Cleaner Product 17: 1025-1029.

43. Wei X, Du X, Chen D, Chen Z (2006) Thermal analysis study of 5,10,15,20-tetrakis (methoxyphenyl) porphyrins and their nickel complexes. Thermochim. Acta 440: 181-187.

44. Kluson P, Drobek M, Kalaji A, Zarubova S, Krysa J, et al. (2008) Singlet oxygen photogeneration efficiencies of a series of phthalocyanines in well-defined spectral regions. J. Photochem. Photobiol A: Chem. 199: 267-273.

45. Gao R, Stark J, Bahnemann DW, Rabani J (2002) Quantum yields of hydroxyl radicalsin illuminated TiO_2 nanocrystallite layers. J. Photochem. Photobiol. A: Chem 148: 387-391.

46. Machado AEH, Franc MD, Velani V, Magnino GA, Velani HMM, et al. (2008) Characterization and evaluation of theefficiency of TiO_2/zinc phthalocyanine nanocomposites as photocatalysts for wastewater treatment using solar irradiation. Int. J. Photoenergy 1-12.

47. Nash T (1953) The colorimetric estimation of formaldehyde by means of the Hantzschreaction. Biochem. J. 55: 416-421.

48. Chaliha S, Bhattacharyya KG (2009) Fe(III), Co(II) and Ni(II) impregnated MCM-41 for wet oxidative destruction of 2,4-dichlorophenol in water. Catal. Today 141: 225-233.

49. Chaliha S, Bhattacharyya KG, Paul P (2008) Catalytic destruction of 4□ chlorophenol in water. Clean, Soil, Air, Water 36: 488-497.

50. Bian W, Song X, Liu D, Zhang J, Chen X (2011) The intermediate products in the degradation of 4-chlorophenol by pulsed high voltage discharge in water. J Hazard Mater 192: 1330-1339.

51. Wu L, Li A, Gao G, Fei Z, Xu S, et al. (2007) Efficient photodegradation of 2,4-dichlorophenol in aqueous solution catalyzed by polydivinylbenzene supported zinc phthalocyanine. J. Mol. Catal. A 269: 183-189.

52. Rao NN, Dubey AK, Mohanty S, Khare P, Jain R, et al. (2003) Photocatalytic degradation of 2-chlorophenol: a study of kinetics, intermediates and biodegradability. J. Hazard. Mater. B 101: 301-314.

53. Konstantinou K, Sakkas VA, Albanis TA (2001) Photocatalytic degradation of the herbicides propanil and molinate over aqueous TiO_2 suspensions: identification of intermediates and the reaction pathway. Appl. Catal. B: Environ 34: 227-239.

54. Serpone N, Lawless D, Terzian R, Meisel D (1992) Electrochemistry in Colloids and Dispersions. VCH, New York, NY, USA, p: 399.